POLITECNICO DI TORINO
Repository ISTITUZIONALE

Comparison of contact parameters measured with two different friction rigs for nonlinear dynamic analysis

Original
Comparison of contact parameters measured with two different friction rigs for nonlinear dynamic analysis / Fantetti, A.; Pennisi, C.; Botto, D.; Zucca, S.; Schwingshackl, C.. - (2020), pp. 2165-2174. (Intervento presentato al convegno 2020 International Conference on Noise and Vibration Engineering, ISMA 2020 and 2020 International Conference on Uncertainty in Structural Dynamics, USD 2020 tenutosi a Leuven, Belgio nel 2020).

Availability:
This version is available at: 11583/2933356 since: 2021-10-20T15:24:29Z

Publisher:
KU Leuven - Departement Werktuigkunde

Published
DOI:

Terms of use:

This article is made available under terms and conditions as specified in the corresponding bibliographic description in the repository

Publisher copyright

(Article begins on next page)

28 March 2024

Comparison of contact parameters measured with two different friction rigs for nonlinear dynamic analysis

A. Fantetti [1], **C. Pennisi** [2], **D. Botto** [2], **S. Zucca** [2], **C. Schwingshackl** [1]
[1] Imperial College London, Department of Mechanical Engineering,
South Kensington Campus, SW72AZ, London, UK
e-mail: **a.fantetti@imperial.ac.uk**

[2] Politecnico di Torino, Department of Mechanical Engineering,
Corso Duca degli Abruzzi, 24, 10129, Torino, Italy

Abstract
The accurate measurement of contact interface parameters is of great importance for nonlinear dynamic response computations since there is a lack of predictive capabilities for such input parameters. Several test rigs have been developed at different institutions, and a series of measurements published, but their reliability remains unknown due to a lack of direct comparisons. To somehow address this issue, a Round-Robin test campaign was performed including the high frequency friction rigs of Imperial College London and Politecnico di Torino. Comparable hysteresis loops were recorded on specimen pairs manufactured from the same batch of raw stainless steel, for a wide range of test conditions, including varying normal loads, sliding distances and nominal areas of contact. Measurements from the two rigs were compared to quantify the level of agreement between the two very different experimental setup, showing a reasonably good matching in the results, but also highlighting some differences. Results also demonstrated that loading conditions can strongly affect the contact parameters, and consequently their effect must be included in future nonlinear dynamic simulations for more reliable predictions.

1 Introduction

In the turbomachinery industry, nonlinear dynamic simulations are required to optimise the design and prevent failures of high value assemblies with friction, such as turbines in aeroengines [1]. To compute those simulations, several contact interface parameters are needed as input. However, due to a lack of predictive capabilities, such parameters need to be accurately measured with purposely designed friction rigs [2-10]. The structural dynamics community has been talking for a long time about comparing contact interface parameters measured from those friction rigs. The comparison is in fact needed to provide more confidence in the data sets used for dynamics simulations of assemblies with friction interfaces.

It is known that friction has a heavy impact on dynamic response [11–15], in terms of shifts in frequency, changes in amplitude and stresses in the structure, which might lead to high cycle fatigue failures of components. The confidence in the measured contact parameters is therefore of importance for more accurate dynamic responses predictions, with the aim of optimising the joint performance (more damping, better repeatability, more robustness), predicting wear, life and the overall nonlinear response of components.

Most of the data for dynamics simulations come from friction rigs that measure hysteresis loops, which are the typical load/displacement curves resulting from contacting interfaces in relative oscillating sliding, see Fig. 1. Such loops are characterised by three regimes, namely the stick regime during the initial phase, the microslip when part of contact starts sliding and the gross slip regime when all of contact is in sliding [2]. Despite their importance for the prediction accuracy, a lack of comparison of experimental data from the existing friction rigs prevents the optimisation of the interfaces for better performance. In fact, while most

hysteresis measurements have been performed at low frequencies [16–20], only few rigs provided measurement data at larger frequencies for dynamics applications [2–7, 21, 22], and a direct comparison between them has never been attempted. For example, there is no standardized approach, although lots of different rigs are available. Hence the idea here to compare quite different rigs to see how comparable the data is, what features are in common and what is different.

A Round-Robin was therefore designed and performed, in which a multitude of comparable hysteresis loops were measured from the friction rigs of Imperial College London (IC) [2] and Politecnico di Torino (PoliTO) [3]. This Round-Robin was designed to directly compare data from such different rigs and to get further insights into the contact behaviour, mapping the contact parameters over a wide range of loading conditions at relatively high frequencies. Preliminary measurements are shown here, with a focus on the comparison of the two different friction rigs to understand how their different designs affect the measurements.

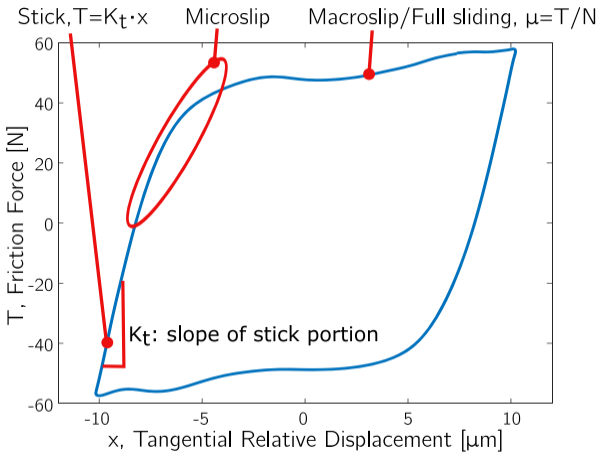


Fig. 1. Typical hysteresis loop [23].

2 Experimental Setup and Round-Robin Description

The two friction rigs are described in detail in [2] for IC and in [3] for PoliTO, and shown in Figs. 2a and 3a. Although the setup of both rigs is quite different, the general idea behind the measurement is very similar. Both rigs generate an oscillating sliding motion between two specimens, one moving and one static. The excitation is harmonic from a shaker, and the relative displacement between the specimens is measured with laser doppler vibrometers very close to the contact interface, so that the bulk deformation effect is minimum, and most of the displacement is due to the sole contact interface. The friction force transmitted between the specimens in contact is measured with dynamic load cells. It is possible to control the relative displacement up to 0.1μm, thanks to the high accuracy of the laser.

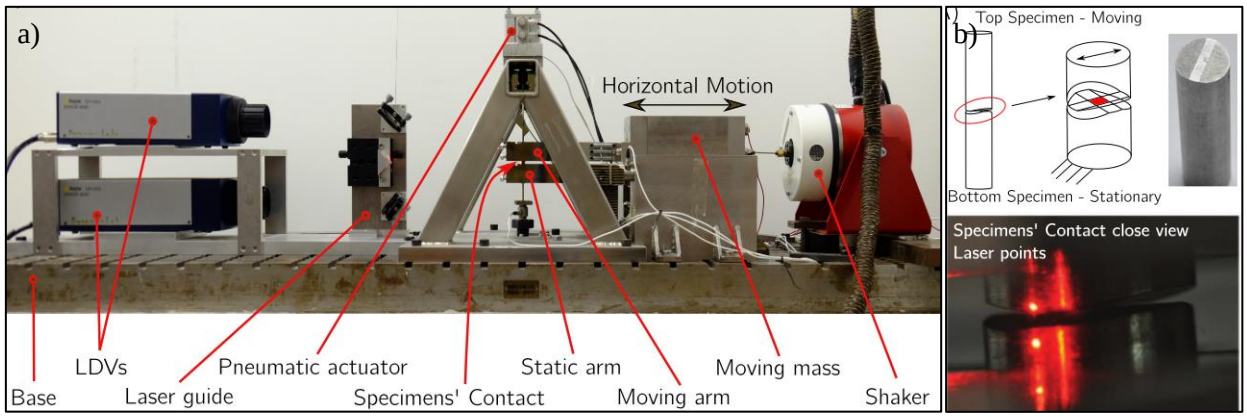


Fig. 2. a) Friction rig at IC; b) IC specimens [2].

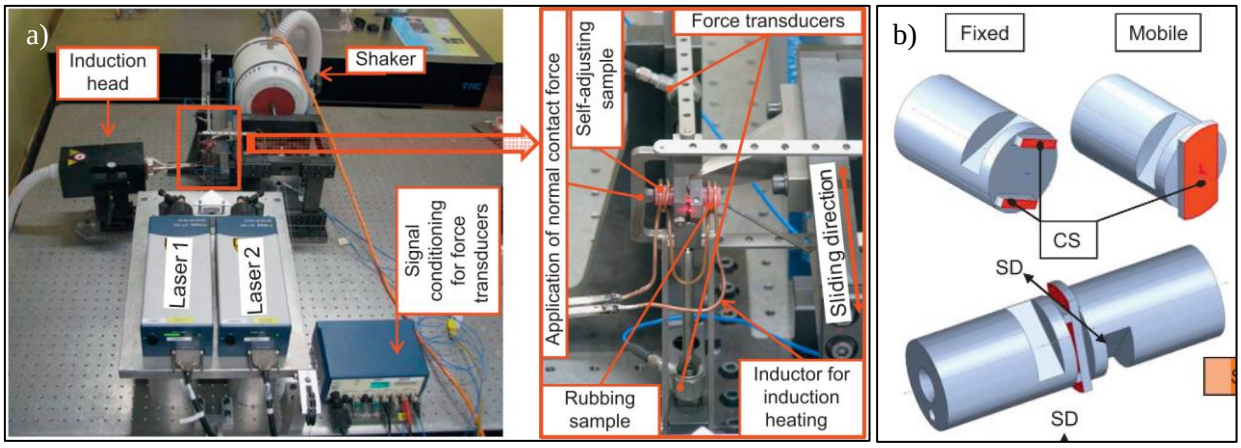


Fig. 3. a) Friction rig at PoliTO; b) PoliTO specimens [3].

These rigs present two main design differences:

- Contact approach: Self-alignment vs rigid alignment. The PoliTO rig employs a novel self-alignment system of the specimens, so that the contact they can always align ensuring a flat contact. Instead the IC rig employs a rigid approach, which requires high tolerance interfaces to guarantee a flat contact.
- Contact geometry: one-leg contact vs two-leg contact. Because of the self-aligning system, PoliTO specimens employ a two-leg contact, as shown in Fig. 3b, while IC rig employs a simpler one patch contact, as shown in Fig. 2b.

These two design differences led to different measurement challenges, which are described in the result section. Finally, Table 1 shows a comparison of the operating regimes of the rigs.

Table 1. Operating regimes of the friction rigs.

	IC	**PoliTO**
Operating frequency	100Hz	175Hz
Displacement amplitude at the operating frequency	0.5-25µm	0.5-50µm
Nominal contact area	1-25mm^2	5-50mm^2
Contact pressure	<500MPa	<30MPa

2.1 Experimental Plan

A test plan was designed to provide a set of input parameters for the community, to compare the quality of data, but also to improve the understanding of the fundamental physics of the contact parameters. Values of friction coefficient and contact stiffness were measured for a wide range of loading conditions, which were chosen based on the compatibility of the rigs, but also to expand the test range beyond what each rig could do. In addition, specimens were manufactured from the same batch of raw 304 stainless steel to guarantee comparability.

The experimental matrix is shown in Fig. 4, and the remaining test conditions are listed in Table 2. For every loading combination, a new specimen pair was used and run for 2.5 consecutive hrs. Although 4 normal loads, 4 displacement amplitudes and 4 nominal areas of contact were chosen, there is overlap only for 10 loading combinations (highlighted in red and green in Fig. 4). The reason is that the two rigs could not

always achieve the same extreme loading conditions because of structural limitations, and therefore it was chosen to keep the central loading values the same and extend the matrix to extreme cases that could only be investigated by one rig. This allowed to explore a larger experimental space.

The range of nominal areas of contact, from 1mm^2 up to 40mm^2, was chosen to check for the scalability of the results, but also to understand what the best way of modelling frictional contacts in dynamics simulations is (e.g. with small or large contact elements). It is worth mentioning that the two rigs operate at different excitation frequencies, which result in different average velocities of the specimens. However, it is expected that the velocity has small effect on the contact parameters compared to the larger variation in the displacement amplitude.

This large experimental matrix and the completion of all the tests resulted in more than 300hrs of testing, with more than 100 different specimen pairs used. A huge amount of data has been obtained and here preliminary results are presented.

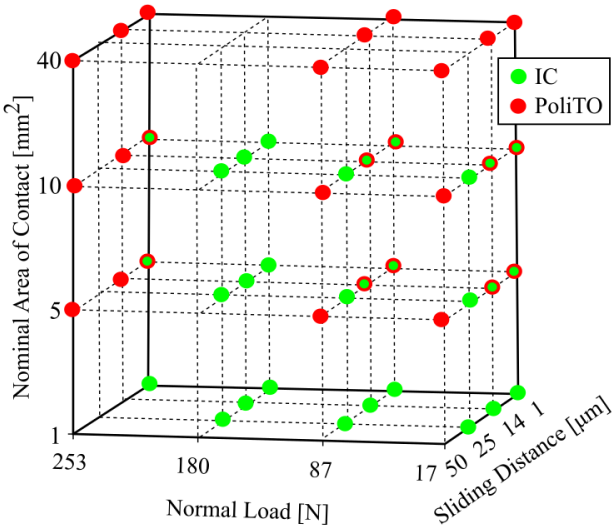


Fig. 4. Test Matrix. Tests with both colours were performed on both rigs.

Table 2. Test matrix summary.

Material	Stainless Steel 304
Type of contact	Flat-on-flat
Temperature	Room Temp.
Excitation Frequency	100 Hz (IC) 175 Hz (PoliTO)
Roughness, R_a	0.1 μm
Running time	2.5 hrs

2.2 Data Post-processing

Both rigs are run continuously for 2.5hrs for each specimen pair, thus generating more than 1.5 million of hysteresis loops per test. Since it is unfeasible to record all those data because of storage limits, only during the first 5 seconds of each test, all the loops were recorded. This was done because hysteresis loops strongly vary at the beginning of the test and consequently a high recording rate is needed to accurately capture their evolution [11]. After the first 5 seconds, loops were recorded with a lower rate until the 50th minute, after which only 10 consecutive hysteresis loops were recorded every 5 minutes. This procedure is reasonably chosen because, after a running-in, a steady state is reached [11].

For every hysteresis loop, the following parameters were extracted:

- Friction Coefficient, calculated with the energy loss formula [3], $E/_{2N\Delta x}$, where E is the energy dissipated within the hysteresis loop, N is the normal load and Δx is the displacement amplitude.
- Tangential contact stiffness, calculated as the gradient of the stick portion of the loop from the reversal up until the force is equal to zero, as shown in Fig. 1.
- Energy Dissipated, evaluated as the area inside the loop, i.e. the integral of the friction force over the relative displacement.

The extraction of the parameters was automatized with a code that read the single hysteresis loops and extracted automatically both friction coefficient and contact stiffness. In addition, scans of the contact interfaces before and after experiments were performed with the Alicona Infinite Focus (Focus Variation) instrument. These scans were used to estimate the worn area of contact with the Mountains® software, by selecting the black worn spots and evaluating their extension.

3 Round-Robin results

In this paper, only preliminary results from the Round-Robin are presented and more will be reported in future publications. Results for a typical test on the IC rig are shown in Fig. 5 (Test n. IC25: 87N normal load, 14µm relative displacement and 5mm^2 nominal area of contact). The evolution of the contact parameters (i.e. friction coefficient and tangential contact stiffness) over the whole test is plotted as a function of the cumulative energy dissipated. This energy is calculated as the sum of the energy dissipated within each hysteresis loop. The friction coefficient (Fig. 5b) rapidly increase within the first cycles as a result of the removal of initial oxide layers on the interfaces, as already observed in [11, 24]. The contact stiffness increases at a slower rate than the friction coefficient, as a result of an increase in the worn area of contact as pointed in previous studies [11]. The larger worn area in fact leads to more asperities and wear scars in contact which contribute to increase the resistance to elastic deformation.

The same behaviour in the friction coefficient is also observed in PoliTO results, as shown in Fig. 6 (Test n. TO14: 87N normal load, 14µm relative displacement and 5mm^2 nominal area of contact). However, on the contrary of what observed in the IC test, the contact stiffness seems to reach a steady state, which is attributed to the approach of the full worn area (as shown in the full worn specimen photo, in contrast with the IC specimen that has not a full worn contact). In fact, although the two tests were run for the same time, only in PoliTO the full worn area was reached, probably because of the self-aligning system, which ensured a full contact, and also because of the larger excitation frequency that led to more cycles in the 2.5hrs and hence to more energy dissipated at the contact (the steady state is reached in PoliTO at around 1500J of energy dissipated, while in IC the test stopped at 1100J). In addition, the PoliTO contact stiffness value is almost 7 times larger than that of IC. This mismatch only occurs because such stiffnesses are not normalised by the worn area of contact, which indeed is larger in PoliTO specimen, as better discussed in Section 4.

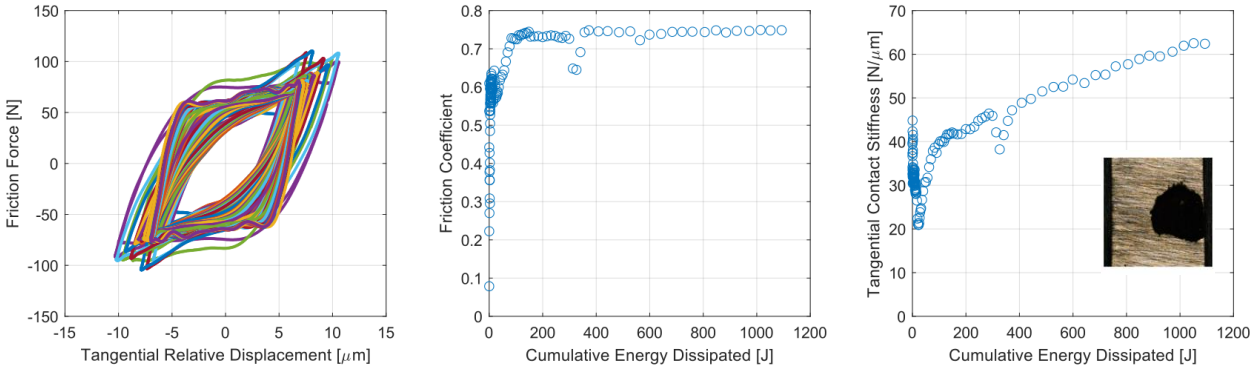


Fig. 5. Typical IC evolution of contact parameters: a) Hysteresis loops; b) Friction coefficient; c) Tangential contact stiffness. Values for the Test n. IC25: 87N normal load, 14µm relative displacement, 5mm^2 nominal area of contact, 100Hz excitation frequency and 2.5hrs of running.

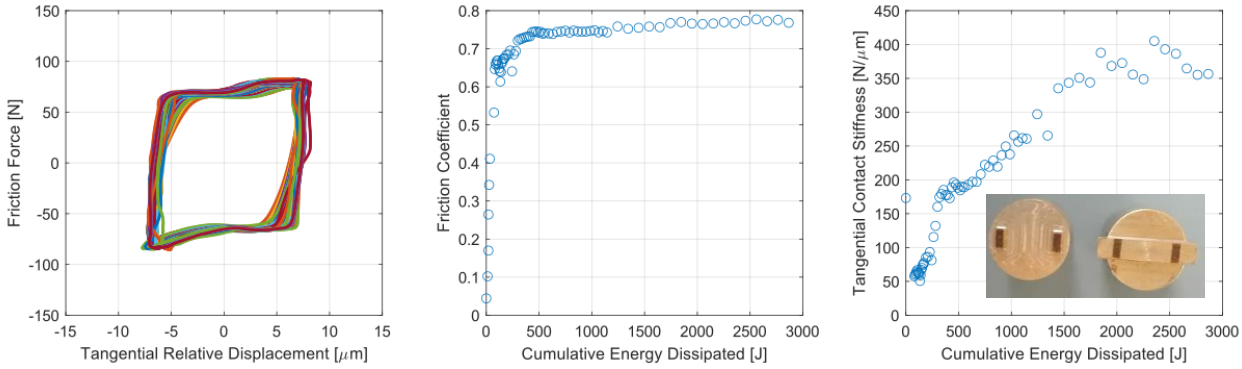
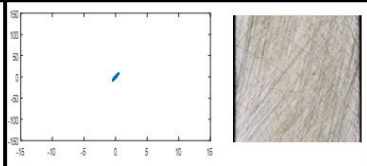
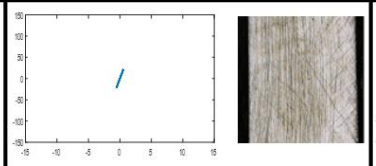
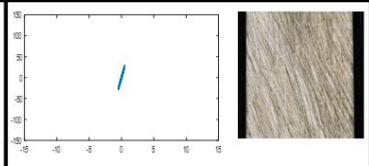
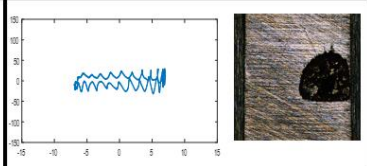
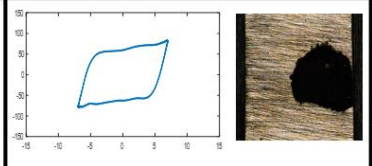
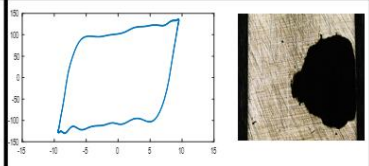
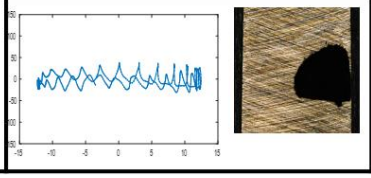
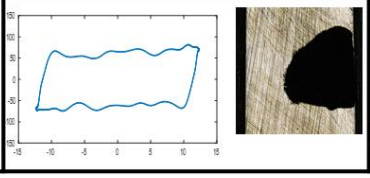
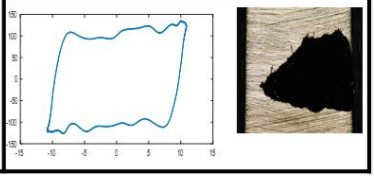


Fig. 6. Typical PoliTO evolution of contact parameters: a) Hysteresis loops; b) Friction coefficient; c) Tangential contact stiffness. Values for the Test n. TO14: 87N normal load, 14µm relative displacement, 5mm^2 nominal area of contact, 175Hz excitation frequency and 2.5hrs of running.

Finally, Table 3 shows an overview of contact interfaces and hysteresis loops for tests conducted on the IC rig on specimens with a 5mm^2 nominal area of contact. During stick tests, at 1µm, there was no energy dissipation, and in fact the hysteresis loops were in a full stuck regime. At larger sliding, loops entered in gross slip. In addition, at very low normal loads (17N), loops that were in gross slip, 14µm and 24.5µm, presented a large amount of oscillations. These oscillations were due to a chattering phenomenon, which occurred when the normal load was so low that specimens were prone to lift-off. In fact, as the normal load increased, this effect disappeared.

The Table also shows the worn area of contact. In the stick tests, 1µm, there was no worn area at the end of the test as a result of the null energy dissipation. At larger sliding distances, the worn area of contact was larger, and it also increased with the normal load, since each loop dissipated more energy at larger normal loads. The same trends were observed in the PoliTO rig, and therefore not shown here for the sake of brevity.

Table 3. Overview of contact interfaces and hysteresis loops for tests conducted on specimens with a 5mm^2 nominal area of contact at IC. Columns are normal loads and rows are displacement amplitudes.

A_{nom}=5mm^2	17N	87N	150N
1µm 0.2mm/s			
14µm 2.8mm/s			
24.5µm 5mm/s			

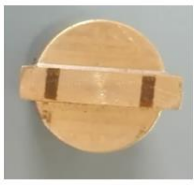
4 Comparison of results

This section compares results obtained from the two friction rigs, discussing matches and differences. To this purpose, Table 4 shows the end-test values for both IC and PoliTO for the 5mm^2 nominal contact area case.

With regards to the contact stiffness, experiments conducted at 1μm of relative displacement show similar values at 17N (difference below the 10%), but at 87N the IC results are by almost 40% larger, probably because of noise due to the very low measured displacement. This might also indicate that PoliTO measurements are affected to a larger extend by the specimen bulk compliance. However, at 14μm of relative displacement, contact stiffness values from the PoliTO rig are larger than those from the IC rig up to 6 times. This occurs only because those values are not normalized by the worn area (which indeed in PoliTO tests is much larger). In fact, after normalizing, contact stiffness values become more comparable, reaching the same order of magnitude with differences below the 40%. This mismatch is reasonably acceptable considering that the two friction rigs have quite different designs. In addition, this relatively close match gives an idea on the amount of uncertainty that different experimental setup can introduce into tests performed at the same loading conditions, although a more detailed study on the uncertainty within each rig will be performed with future analyses. As a result of this contact stiffness comparison, it is concluded that the tangential contact stiffness must be normalized by the worn area of contact to get comparable results, rather than by the nominal area of contact, here the same at IC and PoliTO, as commonly done in the structural dynamics community. However, the challenge is that the worn area is often unknown, because it is not possible to monitor it during experiments, and consequently the system should be run until all of the area wears in, so that a reliable normalization can be performed. Alternatively, the worn area of contact must be determined after each test to establish the normalized stiffness value. Finally, the contact stiffness also increases with the normal load, while it has not a clear trend with the sliding distance because of the final different worn areas of contact achieved (e.g. at 1μm there is no worn area and the contact stiffness is small, while at 25μm the worn area is larger and kt is also larger). Hence, the worn area might hide the influence of the other parameters.

With regards to the friction coefficient, values measured with the PoliTO rig are larger than those from IC by the 3%. It is to be noted that in other tests, here not shown, PoliTO values were larger than IC values up to the 15%. This mismatch can be due to some inaccuracies in the normal load measurement or variations in the normal load during the tests. The friction coefficient also seems to slightly decrease with the increasing normal load.

Table 4. End-test values for the 5mm^2 nominal area of contact. The worn areas of contact at the end of tests performed at 14μm of displacement amplitude are also shown.

A_{nom}=5mm^2	17N		87N	
	IC	PoliTO	IC	PoliTO
1μm	Test IC28 k_t=17N/μm No worn area	Test TO28 k_t=15N/μm No worn area	Test IC30 k_t=40N/μm No worn area	Test TO19 k_t=25N/μm No worn area
14μm	Test IC29 μ=0.79 k_t=39N/μm A_{worn}=0.9mm^2 k_{norm}= 43N/μm/mm^2 	Test TO25 μ=0.81 k_t=72N/μm A_{worn}=2.2mm^2 k_{norm}= 33N/μm/mm^2 	Test IC25 μ=0.75 k_t=63N/μm A_{worn}=1.3mm^2 k_{norm}=49N/μm/mm^2 	Test TO14 μ=0.77 k_t=350N/μm A_{worn}=4.4mm^2 k_{norm}= 79N/μm/mm^2 

In conclusion, despite the two friction rigs show some fundamental design differences (i.e. self-alignment vs rigid alignment, and one-leg contact vs two-leg contact), both measured values and trends are surprisingly comparable, indicating that the overall parameters that are being extracted for use in nonlinear dynamic analysis are most likely accurate enough. Some of the differences in the measurements were attributed to the following differences in the design:

Contact approach, i.e. self-alignment vs rigid alignment:

The two contact approaches employed in the two rigs present different advantages and disadvantages in terms of reliability and repeatability of the results. In the PoliTO rig, more variety of behaviour in the different tests was observed (here not shown) because the rig employed the self-alignment system that strongly depended on the interface morphology and also because larger nominal areas were used, leading to different spots for the initial contact and to different distributions of the worn area of contact. This variety allowed to gain insights into the kinematic dependency of the contact stiffness, since different worn areas were obtained. On the contrary, the IC specimens were rigidly fixed, and this allowed for a better repeatability of the experiments, with similar worn areas of contact achieved after each test. However, because of this rigidity, the IC rig could not employ large areas of contact, because there would be a larger risk of "edge contact" in case of slightly inclined interface, which could not self-align, on the contrary of the PoliTO rig. In fact, as a result of the self-alignment, full worn areas were easily reached in the PoliTO rig, while in the IC rig full worn area could be reached only for the smallest nominal area of contact of $1mm^2$. As a conclusion, the choice on whether using a rigid or self-aligning system depends on the purpose of the test. If more repeatable tests are required, a rigid set up is preferable. However, if more complex and large interfaces are to be tested, a self-aligning system is to be used.

Contact geometry, i.e. one-leg vs two-leg contact:

Two legs are required with a self-aligning system, to avoid tilting. In fact, with a single leg contact, the specimen would tilt unless rigidly fixed. The two-leg design might lead to setup and measurement challenges since the contact is prone to uneven load distribution on the two legs if not mounted accurately. In addition, different results can be obtained depending on which leg is measured and which leg is moving more. The IC setup is easier for mounting instead and leads to more repeatable results, although limitations exist on the size and morphology of the tested interfaces.

5 Conclusions

A test campaign was performed on the high frequency friction rigs at Imperial College London and Politecnico di Torino with the aim to increase the confidence in the measurement of contact interface parameters used as input for nonlinear dynamic analysis of structures with friction joints. To this purpose, a test plan was designed to cover a wide experimental space by testing the friction rigs to their limits and measuring a multitude of hysteresis loops under a range of loading conditions. Specimens had comparable sizes in nominal contact areas and were manufactured from the same batch of raw stainless steel to make the comparison reliable.

Values of friction coefficient and tangential contact stiffness were extracted and compared. Although the two friction rigs presented fundamental design differences, they provided similar values in the measurements. In fact, the friction coefficient showed differences below the 15%, probably coming from noise in the normal and tangential force measurements. The tangential contact stiffness showed discrepancies up to the 50%, which are larger than those observed in the friction coefficient probably because the contact stiffness also depends on displacement measurements, which add more noise in addition to the force measurements. However, this variability is acceptable and these observations increase the confidence in the measured parameters from these rigs, which indeed proved to be quite reliable tools to provide input parameters for nonlinear dynamic simulations, although they can still be improved to further decrease the experimental uncertainty. With regards to the contact parameters, it was shown that the tangential contact stiffness slowly increases during the test because of an increase in the worn area of contact. It is consequently necessary to normalise it by the worn area of contact, rather than by the nominal

area of contact as common practice today. The friction coefficient showed a milder dependency on the loading conditions instead.

These preliminary measurements will be extended once the processing of the very large data set is completed. In fact, more results will be available in future, hopefully providing many more insights for the structural dynamics community and more guidelines on the best use of existing high frequency friction rigs. The authors would also very much like to encourage other research groups to participate in this comparison, so that it can become a comprehensive Round-Robin that will add even more value to the community.

Acknowledgements

This project has received funding from the European Union's Horizon 2020 research and innovation programme under the Marie Sklodowska-Curie grant agreement No 721865.

References

[1] M. Krack, L. Salles, and F. Thouverez, "Vibration Prediction of Bladed Disks Coupled by Friction Joints," *Arch. Comput. Methods Eng.*, vol. 24, no. 3, pp. 589–636, 2017.

[2] A. Fantetti and C. Schwingshackl, "Effect of Friction on the Structural Dynamics of Built-up Structures: An Experimental Study," in *Proceedings of ASME Turbo Expo 2020*, 2020.

[3] M. Lavella, D. Botto, and M. M. Gola, "Design of a high-precision, flat-on-flat fretting test apparatus with high temperature capability," *Wear*, vol. 302, no. 1–2, pp. 1073–1081, 2013.

[4] M. E. Kartal, D. M. Mulvihill, D. Nowell, and D. A. Hills, "Measurements of pressure and area dependent tangential contact stiffness between rough surfaces using digital image correlation," *Tribol. Int.*, vol. 44, no. 10, pp. 1188–1198, 2011.

[5] T. Hoffmann, L. Panning, and J. Wallaschek, "Analysis of Contacts in Friction Damped Turbine Blades Using Dimensionless Numbers," *J. Eng. Gas Turbines Power*, vol. 141, no. 12, Dec. 2019.

[6] A. R. Warmuth, P. H. Shipway, and W. Sun, "Fretting wear mapping: The influence of contact geometry and frequency on debris formation and ejection for a steel-on-steel pair," *Proc. R. Soc. A Math. Phys. Eng. Sci.*, 2015.

[7] J. Hintikka, A. Lehtovaara, and A. Mäntylä, "Fretting-induced friction and wear in large flat-on-flat contact with quenched and tempered steel," *Tribol. Int.*, vol. 92, pp. 191–202, 2015.

[8] D. Botto and M. Lavella, "High temperature tribological study of cobalt-based coatings reinforced with different percentages of alumina," *Wear*, 2014.

[9] M. Umer and D. Botto, "Measurement of contact parameters on under-platform dampers coupled with blade dynamics," *Int. J. Mech. Sci.*, vol. 159, pp. 450–458, Aug. 2019.

[10] M. M. Gola and T. Liu, "A direct experimental-numerical method for investigations of a laboratory under-platform damper behavior," *Int. J. Solids Struct.*, vol. 51, no. 25–26, pp. 4245–4259, Dec. 2014.

[11] A. Fantetti *et al.*, "The impact of fretting wear on structural dynamics: Experiment and simulation," *Tribol. Int.*, vol. 138, pp. 111–124, 2019.

[12] C. Gastaldi, T. Berruti, and M. M. Gola, "The effect of surface finish on the proper functioning of underplatform dampers," *J. Vib. Acoust.*, pp. 1–30, Apr. 2020.

[13] M. R. W. Brake, C. W. Schwingshackl, and P. Reuß, "Observations of variability and repeatability in jointed structures," *Mech. Syst. Signal Process.*, vol. 129, pp. 282–307, Aug. 2019.

[14] T. Butlin, P. Ghaderi, G. Spelman, W. J. B. Midgley, and R. Umehara, “A novel method for predicting the response variability of friction-damped gas turbine blades,” *J. Sound Vib.*, vol. 440, pp. 372–398, Feb. 2019.

[15] S. Bhatnagar, J. Yuan, A. Fantetti, E. Denimal, and L. Salles, “Quantification of Uncertainties in Nonlinear Vibrations of Turbine Blades with Underplatform Dampers,” in *International Conference on Noise and Vibration Engineering*, 2020.

[16] S. Fouvry, T. Liskiewicz, P. Kapsa, S. Hannel, and E. Sauger, “An energy description of wear mechanisms and its applications to oscillating sliding contacts,” *Wear*, vol. 255, no. 1–6, pp. 287–298, 2003.

[17] H. Lee and S. Mall, “Investigation into effects and interaction of various fretting fatigue variables under slip-controlled mode,” *Tribol. Int.*, vol. 39, pp. 1213–1219, 2006.

[18] X. Huang and R. W. Neu, “High-load fretting of Ti-6Al-4V interfaces in point contact,” *Wear*, vol. 265, no. 7–8, pp. 971–978, 2008.

[19] W. Lu *et al.*, “Influence of surface topography on torsional fretting wear under flat-on-flat contact,” *Tribol. Int.*, vol. 109, pp. 367–372, 2017.

[20] V. Done, D. Kesavan, M. Krishna R, T. Chaise, and D. Nelias, “Semi analytical fretting wear simulation including wear debris,” *Tribol. Int.*, vol. 109, pp. 1–9, 2017.

[21] C. H. Hager, J. H. Sanders, and S. Sharma, “Characterization of mixed and gross slip fretting wear regimes in Ti6Al4V interfaces at room temperature,” *Wear*, vol. 257, no. 1–2, pp. 167–180, 2004.

[22] M. Lavella, “Partial-gross slip fretting transition of martensitic stainless steels,” *Tribol. Int.*, vol. 146, Jun. 2020.

[23] L. Pesaresi, A. Fantetti, F. Cegla, L. Salles, and C. W. Schwingshackl, “On the Use of Ultrasound Waves to Monitor the Local Dynamics of Friction Joints,” *Exp. Mech.*, vol. 60, no. 1, pp. 129–141, 2020.

[24] N. P. Suh and H. C. Sin, “The genesis of friction,” *Wear*, vol. 69, no. 1, pp. 91–114, 1981.